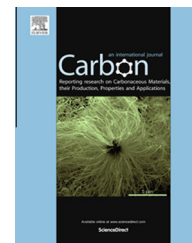


Available at [www.sciencedirect.com](http://www.sciencedirect.com)

ScienceDirect

journal homepage: [www.elsevier.com/locate/carbon](http://www.elsevier.com/locate/carbon)

# Nanoscopic observations of stress-induced formation of graphitic nanocrystallites at amorphous carbon surfaces

Ding-Shiang Wang<sup>a,1</sup>, Shou-Yi Chang<sup>a,\*</sup>, Yi-Chung Huang<sup>a</sup>, Jin-Bao Wu<sup>b</sup>, Hong-Jen Lai<sup>b,\*</sup>, Ming-Sheng Leu<sup>b</sup>

<sup>a</sup> Department of Materials Science and Engineering, National Chung Hsing University, Taichung 40227, Taiwan

<sup>b</sup> Material and Chemical Research Laboratories, Industrial Technology Research Institute, Chutung 30010, Taiwan

## ARTICLE INFO

### Article history:

Received 5 January 2014

Accepted 19 March 2014

Available online 27 March 2014

## ABSTRACT

The formation of graphitic nanocrystallites at the surface of amorphous carbon under large mechanical stresses was examined by using micro-Raman spectrometry, transmission electron microscopy and *in-situ* compressions. In the Raman analyses of severely deformed (above a strain energy density criterion of 5.9 J/m<sup>2</sup>) surface regions of nanoscratched and nanoindented amorphous carbon films, two additional sharp and narrow peaks, D<sub>Gr</sub> and G<sub>Gr</sub> at 1330 and 1580 cm<sup>-1</sup>, appeared from the main unchanged broad spectra, revealing the transformation of some small-range amorphous carbon to nanocrystalline graphite. Transmission electron microscopic images presented the formation of surface shear layer within which dispersed graphitic nanocrystallites (a size of about 3 nm) were formed in the remaining amorphous matrix. The *in-situ* nanoscopic observation of amorphous carbon nanopillars under compressions confirmed the formation of graphitic nanocrystallites at pillar edge surfaces. The formed graphite (001) and (100) lattices were well oriented along maximum resolved shear stresses, being an evidence of lattice reconstruction and suggesting a possibility of stress-induced graphitization of amorphous carbon in the absence of heat.

© 2014 Elsevier Ltd. All rights reserved.

## 1. Introduction

Amorphous carbon (*a*-C), generally including hydrogenated (*a*-C:H), metal-doped (*a*-C:Me) and diamond-like carbon (DLC), has been widely used as surface protective coatings to prevent cutting and machinery tools from severe tribological damages owing to its high hardness and wear resistance, low friction coefficient, high thermal conductivity and good chemical inertness [1–3]. In particular, the low friction coefficient

and a consequent low wear loss are essential to a good tribological performance. The low friction coefficient of *a*-C is most possibly attributed to a self-lubrication behavior owing to the existence of graphite transfer layer on sliding surfaces [3–6]. The surface transfer layer which is composed of so-called amorphous graphite or graphite-like carbon is believed to form via an amorphous-to-crystalline transformation driven by the heat generated by friction and/or the stress provided by the mechanical/friction force [3–11]. However

\* Corresponding authors: Fax: +886 4 22857017 (S.-Y. Chang). Fax: +886 3 5820207 (H.-J. Lai).

E-mail addresses: [shouyi@dragon.nchu.edu.tw](mailto:shouyi@dragon.nchu.edu.tw) (S.-Y. Chang), [hjlai@itri.org.tw](mailto:hjlai@itri.org.tw) (H.-J. Lai).

<sup>1</sup> The authors contributed equally.

<http://dx.doi.org/10.1016/j.carbon.2014.03.035>

0008-6223/© 2014 Elsevier Ltd. All rights reserved.

whether the dominant mechanism for the formation of the transfer layer is based on heat or alternatively on a stress is still doubted although heat has been widely considered to induce the graphitization of *a*-C [12,13].

Previous researches indicated the appearance of friction-induced phase transformation of *a*-C to crystalline graphite at the macroscale [4–6], and most of them suggested that the flash heat on sliding surfaces played the most important role in inducing the graphitization of *a*-C [3,7]. Recent studies by molecular dynamic simulations and *in-situ* electron microscopy attempted to verify any possibility of purely stress-induced phase transformation of *a*-C from a nanoscale perspective, excluding the participation of flash heat [10,11]. Nevertheless, only simulation results or the changes in bonding configurations, rather than a direct nanoscopic observation of graphitic lattice formation or a clear mechanism of purely stress-facilitated graphitization, were discovered. Therefore in this study, micro-Raman analyses and high-resolution transmission electron microscopy (TEM) as well as the *in-situ* TEM analyses of nanopillar deformation under compressions were applied to examine the nanoscopic structure changes of deformed *a*-C and to verify the stress-induced graphitization mechanism in the absence of heat. The study is believed not only to contribute towards better understanding of the mechanistic model of stress-induced graphitization of *a*-C, but also possibly assist in the development of patterned graphite or even graphene on the surface of *a*-C layers for potential applications to transparent conducting devices of ultrahigh wear resistance.

## 2. Experimental

Multilayered *a*-C films (eight layers, each layer 50 nm in thickness) were deposited on Si substrates by a periodic cathodic vacuum arc system [14]. Before the deposition of the *a*-C films, Ti (27 nm) and TiC (120 nm) interlayers were deposited to improve interface adhesion. A UMIS nanoindenter (Base Model, CSIRO) with a Berkovich tip and a scratch module was applied to scratch the *a*-C films at a ramping load from 0 to 400 mN (a scratch length of 2000  $\mu\text{m}$ ; a low and constant moving speed of 50  $\mu\text{m}/\text{s}$  to suppress temperature rise (heat generation) during tip sliding) and to indent the films at a load of 400 mN (loading rate of 0.8 mN/s). Optic and scanning electron microscopes (SEM, JEOL JSM-6700F) were used to observe the surface morphologies of the *a*-C films along the scratch tracks and around the indents. Visible micro-Raman spectroscopy (Horiba Jobin-Yvon LabRAM HR; wavelength of 633 nm, spot size of 3–5  $\mu\text{m}$ ) was applied to detect the bond structures of the *a*-C films at different stages of the scratch tracks and at the center of the indents as schematically plotted in Fig. 1. Multiplex peak fittings of the Raman spectra were performed using a Gaussian–Lorentz function. A high-resolution TEM (JEOL JEM-2100F) was employed to observe the microstructures and lattice structures of the non-deformed and the severely deformed regions (at the end stage of scratch tracks near film fracture) of the *a*-C films. Cross-sectional thin foils for TEM observations were cut from the films (with a top Pt protection layer), as also plotted in Fig. 1, by using a focused ion beam (FIB, FEI Nova 200) at a low current of 50 pA. For

the *in-situ* TEM analyses of *a*-C nanopillars under compressions, the thin *a*-C foils were attached to C-shape rings and further cut into nanopillars (diameter of about 100 nm, length of 1–2  $\mu\text{m}$ , Fig. 1). The *in-situ* TEM compressions were then performed by using the PicoIndenter<sup>®</sup> (Hysitron Inc.) installed in a TEM (JEOL JEM-2010); a flat-top indenter (tip diameter of 1  $\mu\text{m}$ ) was used to compress the nanopillars in a displacement-control mode.

## 3. Results and discussion

### 3.1. Micro-Raman analyses of nanoscratched and nanoindented *a*-C

Fig. 2 (a) shows the optic micrograph of *a*-C film along a nanoscratch track, marked with micro-Raman detecting locations at different stages of the scratch track, and Fig. 2(b) presents the Raman spectra of non-deformed *a*-C film and the deformed regions at the different stages. The spectrum of the non-deformed *a*-C film was broad, the same as the spectra of typical *a*-C structures [1]. At the beginning and central stages, the broad spectra basically remained, indicating no structural changes after slight deformations. However, along the track with higher loads, the spectra were clearly found to vary: two extra small but narrow peaks at the wavenumbers of 1330 and 1580  $\text{cm}^{-1}$  (the positions of the two peaks in the measured spectrum of pure microcrystalline graphite in Fig. 2(c)) additionally appeared from the main unchanged broad spectra, which revealed a possible structural change in some small regions of the severely deformed *a*-C film. From the peak fittings of the Raman spectra shown in Fig. 3, it was much clear that the main broad spectra that combined the overlapped broad D and G bands represented *a*-C [1], while the two separated extra narrow peaks, defined as  $D_{\text{Gr}}$  and  $G_{\text{Gr}}$  (referred to literature [1,15–16] and Fig. 2(c)), indicated the existence of some graphitic nanocrystallites (short-range ordered islands) in the *a*-C matrix. For the non-deformed and the slightly deformed regions (Fig. 3(a) and (b)), the detected spectra mainly consisted of the broad D and G bands [1,12,15] though very small and broad  $D_{\text{Gr}}$  and  $G_{\text{Gr}}$  peaks as an indicator of a trivial amount of intrinsic graphite structure were also included. In comparison, at the end stages of the track in particular near film fracture under large mechanical stresses (Fig. 3(c) and (d)), the two additional  $D_{\text{Gr}}$  and  $G_{\text{Gr}}$  peaks became much stronger in intensity, sharper in shape, and narrower in width, suggesting the transformation of more small regions in the *a*-C matrix into crystalline graphite islands. Though the present spectra that combine a main unchanged broad spectrum (D + G, *a*-C) and two extra narrow peaks (graphitic nanocrystallites) are different from the generally observed ones of large-range, whole-specimen transformed micro- or nanocrystalline graphite [1,17], however they are similar to the ones of small-sized graphitic carbon debris embedded in an amorphous matrix [5,18–19] because the small-range phase transformation is expected to occur only at the highly stressed surface of the scratch tracks [20]. By using the model established for broad spectra by Ferrari and Robertson that  $I_{\text{D}}/I_{\text{G}} = cL_{\text{a}}^2$  ( $c = 4.4$ ) [15], the graphitic domain size,  $L_{\text{a}}$ , of the present *a*-C matrix ( $I_{\text{D}}/I_{\text{G}} = 0.85$ ) was

Download English Version:

<https://daneshyari.com/en/article/7853688>

Download Persian Version:

<https://daneshyari.com/article/7853688>

[Daneshyari.com](https://daneshyari.com)